PCCP

Quaternary mutual diffusion coefficients for aqueous solutions of a cationic–anionic mixed surfactant from moments analysis of Taylor dispersion profiles

Kimberley MacEwan and Derek G. Leaist*

Department of Chemistry, University of Western Ontario, London, Ontario, Canada N6A 5B7. E-mail: dleaist@uwo.ca; Fax: (519) 661-3022; Tel: (519) 661-2166 ext 86317

Received 11th June 2003, Accepted 21st July 2003
First published as an Advance Article on the web 6th August 2003

Taylor dispersion is used to measure mutual diffusion in aqueous solutions of dodecyltrimethylammonium bromide (DTAB) + sodium octanoate (NaOct), a cationic–anionic mixed surfactant. Diffusion of the four different constituent ions (DTA^+, Br^-, Na^+, Oct^-) constrained only by electroneutrality produces three independent solute fluxes. Mutual diffusion in these solutions is therefore a quaternary process described by nine D_{ik} coefficients. Injecting excess DTAB or NaOct into DTAB + NaOct carrier solutions produces remarkable refractive-index profiles with three maxima and two minima. Least-squares analysis of these profiles failed to converge, prompting the development of a procedure for the evaluation of quaternary D_{ik} coefficients from the heights, areas, first moments, and second moments of dispersion profiles. The reported D_{ik} coefficients describe the coupled diffusion of DTAB(1) + NaOct(2) + NaBr(3) components in solutions containing 40 mmol dm^{-3} total surfactant at 25 °C and four different DTAB:NaOct ratios. The results show that the unusual profile shapes are caused by strongly coupled diffusion, as indicated by large negative D_{12}, D_{21} values and large positive D_{32}, D_{31} values which exceed the magnitude of main-coefficients D_{11} and D_{22}. Binary mutual diffusion coefficients for aqueous DTAB solutions and critical micelle concentration for DTAB + NaOct solutions are also reported.

1. Introduction

Several studies[1–11] have drawn attention to the interesting mutual diffusion properties of multicomponent surfactant solutions. For example, mutual diffusion in ternary solutions of an ionic surfactant with an added salt[1] is strongly coupled by the electric field generated by the diffusion of charged micelles and relatively mobile free counterions. Ternary mutual diffusion in surfactant + solubilizate[2–4] solutions, mixed-surfactant[5–8] solutions, and water-in-oil microemulsions[9–11] has also been studied. Transport in these systems is strongly coupled by the formation of mixed micelles or microscopic surfactant-coated water droplets. It is not uncommon for a gradient in the concentration of a surfactant or solubilizate to drive a coupled flux of another component that considerably exceeds its own flux. More remarkably, a recent study has shown that aqueous sodium dodecyl sulfate (NaDS) + dodecylsulfobetaine (DSB) solutions demonstrate "incongruent" diffusion of DSB (negative main D_{ii} diffusion coefficient).[8] This means that a flux of surfactant can be driven from regions of lower surfactant concentration to regions of higher surfactant concentration *by its own concentration gradient*. In addition to fundamental interest, diffusion in multicomponent surfactant solutions plays important roles in the kinetics of solubilization, digestion, emulsification, detergency, tertiary petroleum recovery, and other processes of practical significance.[12,13]

The work reported here is a study of mutual diffusion in aqueous solutions of dodecyltrimethylammonium bromide (DTAB) + sodium octanoate (NaOct), a cationic–anionic mixed surfactant.[14–18] The diffusion of this kind of mixed surfactant was investigated because oppositely-charged surfactant ions can readily form mixed micelles, which might in turn produce unusually strong coupling of the surfactant fluxes. Also, though not immediately obvious, mutual diffusion in cationic–anionic mixed surfactant solutions possesses an extra degree of freedom relative to previously studied ternary surfactant systems. Mutual diffusion in aqueous DTAB + NaOct solutions, for example, produces fluxes of four different constituent ions (DTA^+, Br^-, Na^+, Oct^-) constrained only by electroneutrality, and consequently there are three independent solute fluxes described by nine quaternary mutual diffusion coefficients. (Quaternary mutual diffusion in solutions of two electrolytes without a common ion is discussed in detail in a study of diffusion in aqueous NaCl + $MgSO_4$ and LiCl + NaOH solutions.[19])

In binary aqueous DTAB solutions, DTA^+ and Br^- ions are required to diffuse at the same speed in order to maintain electroneutrality, even though the ions have different mobilities. In aqueous DTAB + NaOct solutions, however, there are more than two constituent ions, so the DTA^+ and Br^- ions can diffuse at different speeds (not as a single DTAB component) without violating the condition of electroneutrality. Similarly, the Na^+ and Oct^- ions in DTAB + NaOct solutions do not diffuse as a single NaOct component. Fluxes of DTAB and NaOct are therefore insufficient to describe mutual diffusion in solutions of these mixed surfactants. The quaternary mutual D_{ik} coefficients for aqueous DTAB + NaOct solutions reported here relate the molar fluxes J_i of total DTAB(1), NaOct(2) and NaBr(3) components to the gradients ∇c_i in the concentrations of these components.

$$J_1(\mathrm{DTAB}) = -D_{11}\nabla c_1 - D_{12}\nabla c_2 - D_{13}\nabla c_3 \quad (1)$$

$$J_2(\mathrm{NaOct}) = -D_{21}\nabla c_1 - D_{22}\nabla c_2 - D_{23}\nabla c_3 \quad (2)$$

$$J_3(\mathrm{NaBr}) = -D_{31}\nabla c_1 - D_{32}\nabla c_2 - D_{33}\nabla c_3 \quad (3)$$

Aqueous DTAB + NaOct solutions were studied because this pair of surfactants is sufficiently soluble to allow diffusion measurements over the entire range of DTAB:NaOct ratios. Although tracer diffusion coefficients[17,18] for cationic–anionic mixed surfactant solutions have been reported previously, no mutual diffusion data appear to be available for this kind of mixed surfactant.

The quaternary D_{ik} coefficients reported here were measured by the Taylor dispersion (peak-broadening) method.[20] In this technique, an initial concentration disturbance is created by injecting a small volume of solution into a laminar carrier stream of slightly different composition at the entrance to a long capillary tube. A differential refractometer (or another suitable detector) monitors the broadened distribution of the injected sample at the tube outlet. The D_{ik} coefficients are evaluated by using a nonlinear least-squares procedure[21,22] to fit the quaternary dispersion equations to the measured dispersion profiles.

The injection of solution samples containing an excess of a single solute relative to the carrier solution usually produces dispersion profiles that resemble Gaussian peaks. Strikingly different profiles were measured for aqueous DTAB + NaOct solutions. As illustrated in Fig. 1, injecting excess NaOct produced highly unusual profiles with five extrema (three peaks and two valleys)! Similar profiles could easily be generated by injecting a solution sample containing simultaneously: (i) a higher concentration of a slowly-diffusing solute to produce a broad dispersion peak; (ii) a higher concentration of rapidly-diffusing second solute to produce a sharp central maximum; (iii) a lower concentration of a third solute diffusing at an intermediate rate to produce the two valleys (see Fig. 2). The profiles shown in Fig. 1 are extraordinary because they were generated by an initial concentration gradient in a single solute component.

The DTAB + NaOct dispersion profiles, though intriguing, proved to be extremely difficult to analyze by nonlinear least-squares procedures. Despite numerous attempts employing a wide range of initial parameter estimates, the fitting failed to converge. Similar difficulties were encountered in a previous study of strongly coupled diffusion in ternary surfactant solutions, prompting the development of an alternate procedure for the evaluation of ternary D_{ik} coefficients from the heights, areas, and first moments of dispersion profiles.[23] In the work reported here, the unusual DTAB + NaOct dispersion profiles are analyzed by developing a procedure for the evaluation of quaternary D_{ik} coefficients from the heights, areas, first moments, and second moments of measured dispersion profiles. The proposed moments analysis is tested for dilute quaternary aqueous solutions of mannitol + glycine + urea. These solutes are non-associating and carry zero electric charge, so the measured main D_{ii} coefficients should be nearly identical to the binary mutual diffusion coefficient for dilute solutions of each solute, and the cross-D_{ik} coefficients ($i \neq k$) should be very small relative to the main coefficients.

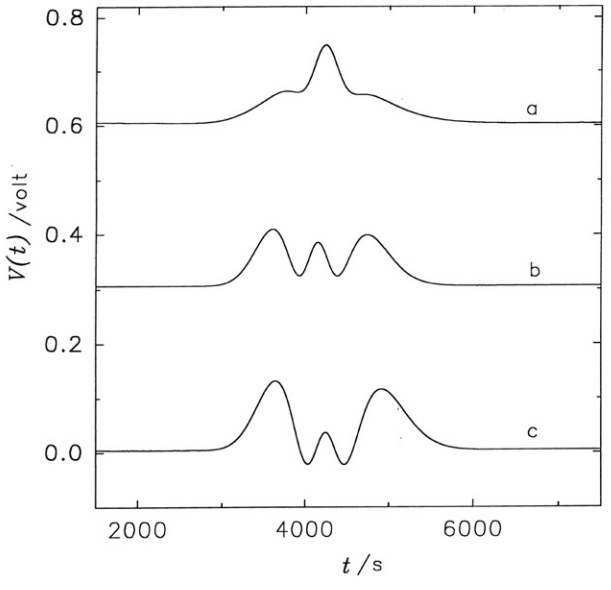

Fig. 1 Dispersion profiles (refractometer detector voltage plotted against time) produced by injecting solution samples containing 20.0 mmol dm^{-1} NaOct into DTAB + NaOct carrier solutions containing: (a) 20.0 mmol dm^{-3} DTAB + 20.0 mmol dm^{-3} NaOct; (b) 30.0 mmol dm^{-3} DTAB + 10.0 mmol dm^{-3} NaOct; (c) 38.0 mmol dm^{-3} DTAB + 2.0 mmol dm^{-3} NaOct. The profiles have been offset for clarity.

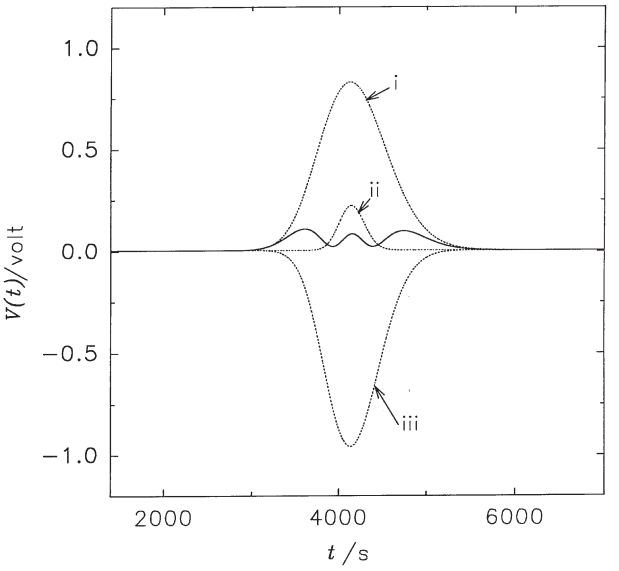

Fig. 2 Dispersion profile (solid curve) produced by injecting a solution sample containing (i) an excess (relative to the carrier solution) of a slowly-diffusing component, (ii) an excess of a rapidly-diffusing component, (iii) a lower concentration of a third component that diffuses at an intermediate rate.

2. Experimental

Procedure

Solutions were prepared by weight by dissolving reagent-grade solutes (Sigma, > 99% purity) in distilled deionized water. Volumetric concentrations were calculated using densities measured with an Anton Paar model DMA 50 density meter (accuracy ± 0.00001 g cm^{-3}). Dispersion profiles were generated by injecting 0.020 cm^3 samples of solution into laminar carrier streams flowing in a Teflon dispersion tube (length 1600 cm, inner radius $r = 0.0406_0$ cm). Retention times t_R were typically 4,000 s to 5,000 s. An HPLC differential-refractometer detector (Hewlett-Packard model 1047A, sensitivity 10^{-8} refractive index units) monitored the dispersion profiles at the tube outlet. Refractometer output voltages $V(t)$ were measured at 5 s intervals by a computer-controlled digital voltmeter (Hewlett-Packard model 3478A).

To help interpret diffusion in the DTAB + NaOct solutions, a few binary mutual diffusion coefficients D were measured for aqueous DTAB solutions. The binary dispersion profiles were analyzed by fitting the equation[24]

$$V(t) = B_0 + B_1 t + V_{max} \sqrt{t_R/t}\, \exp[-12D(t - t_R)^2/r^2 t] \quad (4)$$

to the measured detector voltages, treating the baseline voltage B_0, baseline slope B_1, peak height V_{max}, retention time t_R, and D as adjustable parameters. Mutual diffusion coefficients

for binary aqueous NaOct and NaBr solutions have been reported previously[25,26]

Quaternary dispersion profiles

Quaternary dispersion profiles are generated by injecting a small volume ΔV of solution of composition $\bar{c}_1+\Delta c_1$, $\bar{c}_2+\Delta c_2$, $\bar{c}_3+\Delta c_3$ into a laminar carrier solution of composition $\bar{c}_1$, $\bar{c}_2$, $\bar{c}_3$. The carrier solution flows at mean speed U through a capillary tube of length L and internal radius r. Axial convection and radial diffusion combine to produce the concentration profiles[21,22]

$$c_i(t) = \bar{c}_i + \frac{2\Delta V}{\pi r^3 U}\sqrt{\frac{3}{\pi t}}\sum_{p=1}^{3}\sum_{q=1}^{3} A_{ip}B_{pq}\Delta c_q\sqrt{D_p} \times \exp\left[-\frac{12D_p(t-t_R)^2}{r^2 t}\right] \quad (5)$$

at the tube outlet, a distance $L = t_R U$ downstream from the point of injection. D_1, D_2, D_3 are the eigenvalues of the matrix $\boldsymbol{D}$ of quaternary mutual D_{ik} coefficients and t is the time elapsed since the injection. The columns of matrix $\boldsymbol{A}$ are independent eigenvectors of $\boldsymbol{D}$, and $\boldsymbol{B}$ is the inverse of matrix $\boldsymbol{A}$, all evaluated at the background composition of the carrier stream.

The refractometer detector gives a linear response to the changes in the concentration of each solute across the dispersion profiles

$$V(t) = B_0 + B_1 t + k\sum_{i=1}^{3} R_i\,[c_i(t) - \bar{c}_i] \quad (6)$$

In the notation used here, the change in refractive index n per unit change in the concentration of component i is $R_i = (\partial n/\partial c_i)c_{k\neq i}$ and $k = \mathrm{d}V/\mathrm{d}n$ denotes the detector sensitivity, both evaluated at the composition of the carrier solution. B_1, the baseline slope, is included to allow for small linear drifts in the detector signal.

Combining eqns. (5) and (6) gives

$$V(t) = B_0 + B_1 t + V_{\max}\sqrt{t_R/t}\sum_{p=1}^{3} W_p \exp\left[\frac{12D_p(t-t_r)^2}{r^2 t}\right] \quad (7)$$

for the detector signal across a quaternary dispersion profile. The normalized pre-exponential factors ($W_1+W_2+W_3=1$)

$$W_p = \frac{w_p\sqrt{D_p}}{w_1\sqrt{D_1}+w_2\sqrt{D_2}+w_3\sqrt{D_3}} \quad (8)$$

are related to the initial concentration differences by[22]

$$w_1 = a + b\alpha_1 + d\alpha_2 \quad (9)$$

$$w_2 = e + f\alpha_1 + g\alpha_2 \quad (10)$$

$$w_3 = 1 - w_1 - w_2 \quad (11)$$

where α_1 and α_2 denote the fraction of the refractive index difference generated by the initial concentration difference in component 1 and component 2, respectively.

$$\alpha_1 = \frac{R_1\Delta c_1}{R_1\Delta c_1 + R_2\Delta c_2 + R_3\Delta c_3} \quad (12)$$

$$\alpha_2 = \frac{R_2\Delta c_2}{R_1\Delta c_1 + R_2\Delta c_2 + R_3\Delta c_3} \quad (13)$$

a, b, d, e, f, and g are constants for each carrier solution.

Nonlinear least-squares analysis of quaternary dispersion profiles

Retention times are usually much larger than the widths of typical dispersion peaks. Hence $12D_p(t-t_R)^2/r^2 t \approx 12D_p(t-t_R)^2/r^2 t_R$, and eqn. (7) shows that quaternary dispersion profiles resemble three overlapping Gaussian profiles centred on time t_R with variances $24D_1/r^2 t_R$, $24D_2/r^2 t_R$, and $24D_3/r^2 t_R$. For particular initial conditions satisfying $w_1 = 1$ and $w_2 = 0$, however, the profiles simplify to a single Gaussian in D_1. Solving eqns. (9) and (10) for these particular "eigen" initial conditions gives $\alpha_1^{(1)} = (de-ag+g)/(bg-df)$, $\alpha_2^{(1)} = (af-be-f)/(bg-df)$ and $\alpha_3^{(1)} = 1-\alpha_1^{(1)}-\alpha_2^{(1)}$ for the fraction of the initial refractive-index difference contributed by each component. An eigenvector of the matrix $\boldsymbol{D}$ with eigenvalue D_1 is therefore obtained by transposing $(\alpha_1^{(1)}/R_1, \alpha_2^{(1)}/R_2, \alpha_3^{(1)}/R_3)$ into a column vector. The corresponding eigenvectors of $\boldsymbol{D}$ with eigenvalues D_2 and D_3, the transposes of $(\alpha_1^{(2)}/R_1, \alpha_2^{(2)}/R_2, \alpha_3^{(2)}/R_3)$ and $(\alpha_1^{(3)}/R_1, \alpha_2^{(3)}/R_2, \alpha_3^{(3)}/R_3)$, are obtained by solving eqns. (9) and (10) for $w_1 = 0$, $w_2 = 1$ and $w_1 = 0$, $w_2 = 0$, respectively, which gives: $\alpha_1^{(2)} = (de-ag-d)/(bg-df)$, $\alpha_2^{(2)} = (af-be+b)/(bg-df)$ and $\alpha_1^{(3)} = (de-ag)/(bg-df)$, $\alpha_2^{(1)} = (af-be)/(bg-df)$.

Quaternary D_{ik} coefficients can be evaluated by using nonlinear least-squares procedures to fit eqn. (7) to sets of three or more dispersion profiles. A typical set of fitted profiles is obtained by injecting excess solute 1 ($\alpha_1 = 1$, $\alpha_2 = 0$), excess solute 2 ($\alpha_1 = 0$, $\alpha_2 = 1$), or excess solute 3 ($\alpha_1 = 0$, $\alpha_2 = 0$) into each carrier solution. B_0, B_1, $V_{\max}$, and t_R are treated as adjustable least-square parameters for each profile, together with the eigenvalues D_1, D_2, D_3 and a, b, d, e, f, g for each set of profiles. In previous studies, the fitting procedure converged rapidly using the pseudo-binary approximation $D_{ik} \approx 0$ for $i \neq k$ and the corresponding initial parameter estimates $a \approx 0$, $b \approx 1$, $d \approx 0$, $e \approx 0$, $f \approx 0$, $g \approx 1$, and $D_i \approx r^2 t_R \ln 2/(3\sigma_i 2)$, where σ_i is the width at half height of the profile generated by injecting excess solute i into the carrier solution. The quaternary D_{ik} coefficients are evaluated by using the similarity transform

$$\boldsymbol{D} = \boldsymbol{A}\begin{bmatrix} D_1 & 0 & 0 \\ 0 & D_2 & 0 \\ 0 & 0 & D_3 \end{bmatrix}\boldsymbol{A}^{-1} \quad (14)$$

where the columns of matrix $\boldsymbol{A}$ defined by $A_{ik} = \alpha_i^{(k)}/R_i$ are the eigenvectors of $\boldsymbol{D}$.

Mutual diffusion coefficients change rapidly in the region of the critical micelle concentration (c.m.c.).[27,28] To maintain essentially constant D_{ik} coefficients across the DTAB + NaOct dispersion profiles, both the carrier solutions and the injected solutions were kept above the c.m.c. This was confirmed by using an Orion model 60 conductivity meter and a no. 1060 electrode to measure ionic conductivities for a series of solutions at fixed DTAB:NaOct ratios prepared by dilution with added water. C.m.c. values were estimated from the break in the plot of molar ionic conductivity against the square root of the total surfactant concentration.

Obtaining reasonable estimates for the initial fitting parameters proved to be extremely difficult for the DTAB + NaOct profiles, especially for the profiles with five extrema illustrated in in Fig. 1. Also, the fitting procedure frequently locked onto a local minimum, another consequence of the complicated profile shapes. For these reasons, nonlinear least-squares analysis of the DTAB + NaOct dispersion profiles failed to converge, despite a large number of fitting attempts.

Moments analysis of quaternary dispersion profiles

Previous work has shown that ternary D_{ik} coefficients can be reliably evaluated from the heights, areas, and first temporal

moments of dispersion profiles, without resorting to nonlinear least-squares fitting procedures[23] In this section, the moments analysis procedure is extended to evaluate quaternary D_{ik} coefficients from the heights, areas, first moments and second moments of dispersion profiles in order to analyze the interesting DTAB + NaOct results.

The first step is to calculate the detector voltages ${}^{E}V(t)$ relative to the baseline.

$$ {}^{E}V(t) = V(t)B_0B_1^t \tag{15}$$

The baseline parameters B_0 and B_1 can be evaluated in practice by using linear least-squares to fit the straight line $B_0 + B_1t$ to baseline voltages selected from the "flat" portions of the leading and trailing edge of each dispersion profile. A more objective procedure for establishing the baseline is described in the Appendix.

The height H, area I_0 (zeroth moment), first moment I_1, and second moment I_2 of a dispersion profile are defined as follows

$$H = {}^{E}V(t_R) \tag{16}$$

$$I_0 = \int_{-\infty}^{+\infty} {}^{E}V(t)\mathrm{d}\,t \tag{17}$$

$$I_1 = \int_{-\infty}^{+\infty} {}^{E}V(t)|t - t_R|\,\mathrm{d}\,t \tag{18}$$

$$I_2 = \int_{-\infty}^{+\infty} {}^{E}V(t)(t - t_R)^2\mathrm{d}\,t \tag{19}$$

The evaluation of D_{ik} coefficients is simplified[23,29] by defining the "reduced" peak heights H', first moments I_1', and second moments I_2'

$$H' = \sqrt{\frac{\pi r^2 t_R}{12}}\frac{H}{I_0} = P + Q\alpha_1 + S\alpha_2 \tag{20}$$

$$I_1' = \sqrt{\frac{12\pi}{r^2 t_R}}\frac{I_1}{I_0} = E + F\alpha_1 + G\alpha_2 \tag{21}$$

$$I_2' = \frac{24}{r^2 t_R}\frac{I_2}{I_0} = X + Y\alpha_1 + Z\alpha_2 \tag{22}$$

which are linear functions of α_1 and α_2. The parameters P, Q, S, E, F, G, X, Y, Z are conveniently evaluated for a given carrier solution by using linear least squares to fit eqns. (20)–(22) to values of H', I'_1, and I'_2 measured for three or more profiles for different values of α_1 and α_2.

For the "eigen" initial conditions $\alpha_1^{(i)}$, $\alpha_2^{(i)}$, $\alpha_3^{(i)}$ defined in the preceding section, the reduced heights, first moments, and second moments give the eigenvalue D_i raised to the powers $\frac{1}{2}$, $-\frac{1}{2}$, and -1, respectively[23,29]

$$P + Q\alpha_1^{(i)} + S\alpha_2^{(i)} = \sqrt{D_i} \tag{23}$$

$$E + F\alpha_1^{(i)} + G\alpha_2^{(i)} = \frac{1}{\sqrt{D_i}} \tag{24}$$

$$X + Y\alpha_1^{(i)} + Z\alpha_2^{(i)} = \frac{1}{D_i} \tag{25}$$

To evaluate the nine quaternary D_{ik} coefficients from the nine parameters P through Z, a simple one-dimensional search procedure was used to solve eqns. (23)–(25) for $\alpha_1^{(i)}$, $\alpha_2^{(i)}$, and D_i. Starting with the trial value $D_i = 0$ (the eigenvalues of D cannot be negative) and increasing the trial D_i value in small increments (*e.g.*, 0.001×10^{-5} cm^2 s^{-1}), eqns. (23) and (24) were used to calculate the corresponding trial values of $\alpha_1^{(i)}$, $\alpha_2^{(i)}$. Eqns. (24) and (25) were then used to evaluate a second set of trial $\alpha_1^{(i)}$, $\alpha_2^{(i)}$ values for the same D_i value. When the differences between the two sets of trial $\alpha_1^{(i)}$, $\alpha_2^{(i)}$ values reached a minimum, Newtons's method was used to calculate accurate values of $\alpha_1^{(1)}$, $\alpha_2^{(1)}$, and D_1. This procedure was repeated for larger trial D_i values to calculate $\alpha_1^{(2)}$, $\alpha_2^{(2)}$, D_2 and $\alpha_1^{(3)}$, $\alpha_2^{(3)}$, D_3. The quaternary D_{ik} coefficients were then evaluated using eqn. (14).

A simple procedure for the evaluation of H, I_0, I_1, and I_2 from the measured detector voltages is given in the Appendix together with other numerical details of the quaternary moments analysis. As a test, quaternary D_{ik} coefficients were measured for a dilute aqueous mannitol(1) + glycine(2) + urea(3) solutions containing 20 mmol dm^{-3} of each solute. Table 1 gives the average D_{ik} coefficients evaluated from six different sets of profiles. Each data set consisted of three profiles generated by an initial concentration difference in mannitol ($\Delta c_1 = 20$ mmol dm^{-3}), glycine ($\Delta c_2 = 20$ mmol dm^{-3}), or urea ($\Delta c_3 = 20$ mmol dm^{-3}). Consistent with the pseudo-binary approximation for dilute solutions of non-interacting solutes, the measured main D_{ii} coefficients agree within experimental error with the binary mutual diffusion coefficient of each solute at a concentration of 20 mmol dm^{-3} (0.662×10^{-5}, 1.057×10^{-5}, and 1.380×10^{-5} cm^2 s^{-1}, respectively).[30–32] Also, the measured cross-D_{ik} coefficients are very small (<3% of the main D_{ii} coefficients).

3. Results

Quaternary mutual diffusion coefficients were measured for aqueous DTAB + NaOct solutions containing 40 mmol dm^{-3} total surfactant at 25 °C and DTAB solute fractions of 0.050, 0.500, 0.750 and 0.950. The injected solution samples contained $\leqslant$ 20.0 mmol dm^{-3} excess DTAB, NaOct, or NaBr relative to the carrier solution. Within this range the measured D_{ik} values were independent of the initial concentration differences and therefore represented differential coefficients at the composition of the carrier solution. The total surfactant concentrations for each carrier solution and injected solutions was at least 20 mmol dm^{-3} above the c.m.c. (see Table 2).

Table 3 gives the average values of the P, Q, S, E, F, G, X, Y, Z parameters from linear least-squares analysis (eqns. (20)–(22)) of the reduced heights, areas, and second moments of four to eight different sets of dispersion profiles for each carrier solution. The corresponding values of $\alpha_1^{(i)}$, $\alpha_2^{(i)}$, and D_i obtained by solving (eqns. (23)–(25)) are listed in Table 4.

Table 1 Quaternary D_{ik} coefficients[a] from moments analysis for aqueous mannitol ($\bar{c}_1 = 20$ mmol dm^{-3}) + glycine ($\bar{c}_2 = 20$ mmol dm^{-3}) + urea ($\bar{c}_3 = 20$ mmol dm^{-3}) solutions (25 °C)

i	$D_{i1}/10^{-5}$ cm^2 s^{-1}	$D_{i2}/10^{-5}$ cm^2 s^{-1}	$D_{i3}/10^{-5}$ cm^2 s^{-1}
1	0.66 (0.02)	0.001 (0.001)	0.00 (0.01)
2	0.01 (0.05)	1.06 (0.02)	0.01 (0.02)
3	0.02 (0.04)	−0.02 (0.01)	1.35 (0.06)

[a] Precision quoted as two standard deviations (in parentheses).

Table 2 Critical micelle concentrations of aqueous DTAB(1) + NaOct(2) solutions at 25 °C

$\bar{c}_1/(\bar{c}_1 + \bar{c}_2)$	$\bar{c}_{1\mathrm{c.m.c.}}$/ mmol dm^{-3}	$\bar{c}_{2\mathrm{c.m.c.}}$/ mmol dm^{-3}	c.m.c./ mmol dm^{-3}
0.000	0.0	350	350
0.050	0.9	17.0	17.9
0.250	2.5	7.5	10.0
0.500	3.9	3.9	7.8
0.750	2.2	6.5	8.7
1.000	15.9	0.0	15.9

Table 3 Parameters from moments analysis of aqueous DTAB ($\bar{c}_1$) + NaOct($\bar{c}_2$) + NaBr($\bar{c}_3 = 0$) solutions at 25 °C

$\bar{c}_1$/mmol dm^{-3}	2	20	30	38
$\bar{c}_2$/mmol dm^{-3}	38	20	10	2
R_2/R_1	0.587 (0.018)	0.568 (0.010)	0.525 (0.002)	0.524 (0.004)
R_3/R_1	0.305 (0.007)	0.293 (0.005)	0.306 (0.002)	0.302 (0.003)
$P/(10^{-5}$ cm^2 s$^{-1})^{1/2}$	1.234 (0.007)	−1.417 (0.044)	1.388 (0.01)	0.349 (0.004)
$Q/(10^{-5}$ cm^2 s$^{-1})^{1/2}$	−1.029 (0.002)	−0.89 (0.04)	−0.782 (0.009)	0.825 (0.005)
$S/(10^{-5}$ cm^2 s$^{-1})^{1/2}$	−1.323 (0.007)	−0.96 (0.04)	−1.121 (0.010)	0.40 (0.04)
$E/(10^{-5}$ cm^2 s$^{-1})^{-1/2}$	0.825 (0.034)	0.37 (0.11)	0.40 (0.04)	0.47 (0.03)
$F/(10^{-5}$ cm^2 s$^{-1})^{-1/2}$	3.34 (0.12)	2.20 (0.13)	1.23 (0.05)	0.41 (0.03)
$G/(10^{-5}$ cm^2 s$^{-1})^{-1/2}$	0.32 (0.04)	2.94 (0.28)	3.64 (0.04)	0.98 (0.03)
$X/(10^{-5}$ cm^2 s$^{-1})^{-1}$	0.74 (0.11)	0.91 (0.83)	0.75 (0.22)	0.55 (0.19)
$Y/(10^{-5}$ cm^2 s$^{-1})^{-1}$	15.2 (1.2)	9.2 (1.6)	3.30 (0.29)	3.99 (0.19)
$Z/(10^{-5}$ cm^2 s$^{-1})^{-1}$	0.79 (.014)	13.1 (1.2)	14.3 (1.8)	21.2 (0.2)

The average D_{ik} values for each composition from moments analysis are listed in Table 5 and are plotted in Fig. 3 against the solute fraction of DTAB, $f_1 = \bar{c}_1/(\bar{c}_1 + \bar{c}_2 + \bar{c}_3)$. The main D_{ii} coefficients are positive at all compositions. Thus incongruent diffusion was not observed. Several attempts were made to measure D_{ik} coefficients at DTAB solute fractions in the range $0.15 \leqslant f_1 \leqslant 0.35$. In this composition region, however, eigenvalues D_2 and D_3 were too close together to be resolved by the moments analysis procedure.

4. Discussion

Diffusion driven by DTAB(1) concentration gradients

The main coefficient D_{11} gives the flux of the total DTAB component (J_1) produced by the gradient in the concentration of the total DTAB component (∇c_1). In the limit $f_1 \rightarrow 1$, D_{11} is the binary mutual diffusion coefficient of aqueous DTAB (the right intercept in Fig. 3). Linear extrapolation of the D_{11} values measured at 0.75 and 0.95 DTAB solute fractions gives $D_{11}(f_1 = 1.00) \approx 0.25 \times 10^{-5}$ cm^2 s^{-1}. This estimate is consistent with the measured binary mutual diffusion coefficient for 40.0 mmol dm^{-3} aqueous DTAB, 0.24×10^{-5} cm^2 s^{-1}. At the other composition extreme, the left intercept in Fig. 3 ($f_1 = 0$), D_{11} is the tracer diffusion coefficient of the DTA$^+$ ion in aqueous NaOct solutions. If all of the DTA$^+$ ions diffuse in micellar form, then the extrapolation of D_{11} to $f_1 = 0$ would give the diffusion coefficient of the micelles. For the DTAB + NaOct solutions, however, this extrapolation is impractical because the limiting solution composition (40.0 mmol dm^{-3} NaOct) drops below the c.m.c. of binary aqueous NaOct (350 mmol dm^{-3}).[33]

Cross-coefficient D_{21} is a measure of the coupled flux of the NaOct(2) component produced by a gradient in the concentration of the DTAB(1) component. At low DTAB solute fractions, D_{21} is negative and relatively large, as shown in Fig. 3. At $f_1 = 0.050$, for example, D_{21} is 8 times larger than D_{11}, indicating that a DTAB concentration gradient produces a counter-flow of 8 mol NaOct per mole of DTAB. Added DTAB, by strongly promoting the formation of mixed micelles, removes free Oct$^-$ ions from solution. The resulting diffusion of free Oct$^-$ ions "up" the DTAB gradient is the likely mechanism for the counter-transport of NaOct caused by DTAB gradients. Similar counter-current coupled flows have been reported for other mixed surfactant solutions.[6,7]

Cross-coefficient D_{31}, in contrast to D_{21}, is large and positive at low DTAB(1) solute fractions. At $f_1 = 0.050$, D_{31} is in fact 15 times larger than D_{11}, which means that 15 moles of NaBr(3) are co-transported per mole of DTAB. This behavior can be understood, at least qualitatively, in terms of the large mobility of the Br$^-$ ions relative to the slower DTA$^+$ ions which diffuse primarily in micellar form.[17] The solutions considered here contain more than two constituent ions. Consequently, the DTA$^+$ ions and the more mobile Br$^-$ ions are not required to diffuse together as a single DTAB component to maintain electroneutrality along the diffusion path, and the flux of Br$^-$ ions exceeds the flux of DTA$^+$ ions produced by a DTAB concentration gradient. The excess flux of total Br$^-$ ions (j_{Br^-}) relative to the flux of total DTA$^+$ ions (j_{DTA^+}) produced by a DTAB concentration gradient equals the co-current coupled flux of the NaBr component: $J_3(\text{NaBr}) = j_{Br^-} - j_{DTA^+}$. This mechanism allows DTAB concentration gradients to produce coupled flows of NaBr in DTAB($\bar{c}_1$) + NaOct($\bar{c}_2$) solutions, even though the solutions contain no added NaBr($\bar{c}_3 = 0$).

Although DTAB concentration gradients produce large coupled flows of NaOct and NaBr components at low DTAB solute fractions, it is impossible to have coupled transport of NaOct or NaBr in solutions that do not contain Na$^+$ ions.

Table 4 Eigenvalues D_1, D_2, D_3 and $\alpha_1^{(i)}$, $\alpha_2^{(i)}$ parameters[a] from moments analysis of aqueous DTAB ($\bar{c}_1$) + NaOct($\bar{c}_2$) + NaBr($\bar{c}_3 = 0$) 0) solutions at 25 °C

$\bar{c}_1$/mmol dm^{-3}	2	20	30	38
$\bar{c}_2$/mmol dm^{-3}	38	20	10	2
$D_1/10^{-5}$ cm^2 s^{-1}	0.073 (0.06)	0.07 (0.02)	0.20 (0.04)	0.172 (0.005)
$D_2/10^{-5}$ cm^2 s^{-1}	0.84 (0.04)	0.62 (0.15)	0.27 (0.07)	0.24 (0.01)
$D_3/10^{-5}$ cm^2 s^{-1}	1.65 (0.16)	1.32 (0.14)	1.39 (0.07)	1.37 (0.05)
$\alpha_1^{(1)}$	0.81 (0.04)	0.57 (0.12)	0.94 (0.04)	0.949 (0.005)
$\alpha_2^{(1)}$	0.39 (0.03)	0.66 (0.12)	0.17 (0.07)	0.121 (0.008)
$\alpha_1^{(2)}$	−0.02 (0.01)	2.11 (0.06)	0.08 (0.09)	0.985 (0.003)
$\alpha_2^{(2)}$	1.04 (0.04)	0.27 (0.07)	0.75 (0.22)	0.04 (0.01)
$\alpha_1^{(3)}$	0.00 (0.02)	0.64 (0.27)	0.18 (0.06)	0.17 (0.05)
$\alpha_2^{(3)}$	−0.12 (0.15)	0.27 (0.13)	0.06 (0.02)	0.03 (0.01)

[a] Precision quoted as two standard deviations (in parentheses).

Table 5 Quaternary mutual diffusion coefficients[a] for aqueous DTAB ($\bar{c}_1$) + NaOct($\bar{c}_2$) + NaBr($\bar{c}_3 = 0$) solutions at 25 °C from moments analysis

$\bar{c}_1$/mmol dm^{-3}	2	20	30	38
$\bar{c}_2$/mmol dm^{-3}	38	20	10	2
$D_{11}/10^{-5}$ cm^2 s^{-1}	0.083 (0.019)	0.50 (0.11)	0.33 (0.02)	0.267 (0.002)
$D_{12}/10^{-5}$ cm^2 s^{-1}	−0.009 (0.006)	−0.04 (0.08)	−0.24 (0.06)	0.311 (0.015)
$D_{13}/10^{-5}$ cm^2 s^{-1}	0.004 (0.009)	0.24 (0.15)	0.09 (0.02)	0.08 (0.02)
$D_{21}/10^{-5}$ cm^2 s^{-1}	−0.66 (0.22)	−0.43 (0.16)	0.03 (0.02)	0.0075 (0.002)
$D_{22}/10^{-5}$ cm^2 s^{-1}	0.83 (0.04)	0.16 (0.13)	0.20 (0.04)	0.166 (0.012)
$D_{23}/10^{-5}$ cm^2 s^{-1}	−0.06 (0.09)	−0.20 (0.22)	0.05 (0.02)	0.024 (0.012)
$D_{31}/10^{-5}$ cm^2 s^{-1}	1.22 (0.43)	0.47 (0.09)	0.10 (0.06)	0.001 (0.007)
$D_{32}/10^{-5}$ cm^2 s^{-1}	0.05 (0.06)	0.64 (0.07)	1.01 (0.11)	1.14 (0.16)
$D_{33}/10^{-5}$ cm^2 s^{-1}	1.66 (0.16)	1.34 (0.12)	1.34 (0.05)	1.35 (0.04)

[a] Precision quoted as two standard deviations (in parentheses).

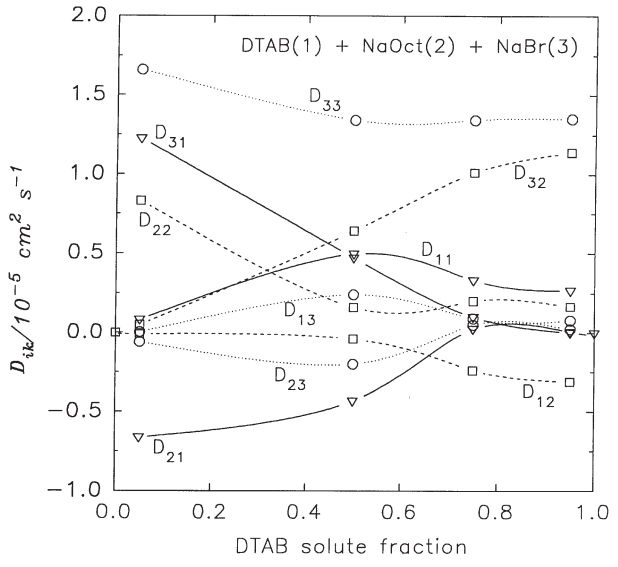

Fig. 3 Quaternary mutual diffusion coefficients of aqueous DTAB ($\bar{c}_1$) + NaOct($\bar{c}_2$) + NaBr($\bar{c}_3 = 0$) solutions at 25 °C from moments analysis of Taylor dispersion profiles.

Consequently, D_{21} and D_{31} are both zero in the limiting case of a binary aqueous DTAB solution ($f_1 = 1.00$ in Fig. 3).

Diffusion driven by NaOct(2) concentration gradients

In the limit $f_1 \rightarrow 0$, main-coefficient D_{22} is the binary mutual diffusion coefficient of aqueous NaOct. The measured D_{22} value at $f_1 = 0.050$ is 0.84×10^{-5} cm^2 s^{-1}, which is very close to binary mutual diffusion coefficient for 40 mmol dm^{-3} aqueous NaOct (0.81×10^{-5} cm^2 s^{-1}).[25] In the limit $f_1 \rightarrow 1$, D_{22} is the tracer diffusion coefficient for Oct$^-$ ions in DTAB solutions. Linear extrapolation of the measured D_{22} values gives 0.15×10^{-5} cm^2 s^{-1} for the tracer coefficient of Oct$^-$ ions in a 40 mmol dm^{-3} DTAB solution. Because this composition is above the c.m.c., the tracer Oct$^-$ diffusion coefficient is the average of the diffusion coefficients of the free Oct$^-$ ions ($D_{\mathrm{Oct}-}$) and the DTAB micelles (D_{mic}) weighted in proportion to the fractions of free Oct$^-$ ions (α) and micellar Oct$^-$ ions ($1 - \alpha$).

$$D_{22}(f_1 = 1.00) = \alpha D_{\mathrm{oct}-} + (1 - \alpha) D_{\mathrm{mic}} \qquad (26)$$

Solving eqn. (26) using the extrapolated D_{22} value together with previously reported estimates of the diffusion coefficients of the free Oct$^-$ ions (0.61×10^{-5} cm^2 s^{-1})[28] and DTAB micelles (0.09×10^{-5} cm^2 s^{-1}) gives $\alpha = 0.88$. Therefore, about 90% of the tracer octanoate ions diffuse in micellar form in a 40 mmol dm^{-3} DTAB solution. The diffusion coefficient of the DTAB micelles was estimated by fitting the chemical equilibrium model[27] for the binary diffusion of an ionic surfactant to the measured D values listed in Table 6. Details of this procedure are given in ref. 27.

NaOct concentration gradients, like DTAB gradients, can drive large coupled flows, especially at low NaOct solute fractions. In particular, the measured D_{12} and D_{32} values at 0.05 NaOct solute fraction ($f_1 = 0.95$) indicate that a NaOct concentration gradient drives a counter-flow of 2 mol DTAB and a co-current flow of 7 mol NaBr per mole of diffusing NaOct. At high NaOct fractions, in contrast, D_{12} and D_{32} are negligibly small because coupled flows of DTAB and NaBr must vanish for solutions that contain no Br$^-$ ions. The coupled flows produced by DTAB concentration gradients are larger than the corresponding coupled flows produced by NaOct gradients because Br$^-$ counterions are more mobile than Na$^+$ counterions.[34] Also, added DTAB, by virtue of its lower c.m.c., more strongly promotes the formation of mixed micelles.

Table 6 Binary mutual diffusion coefficients of aqueous DTAB(1) solutions at 25 °C

$\bar{c}_1$/mmol dm^{-3}	$D/10^{-5}$ cm^2 s^{-1}	$\bar{c}_1$/mmol dm^{-3}	$D/10^{-5}$ cm^2 s^{-1}
5.00	0.88	25.0	0.19
8.01	0.88	30.1	0.21
11.0	0.86	35.0	0.22
14.0	0.84	45.0	0.26
15.0	0.28	60.0	0.31
20.0	0.18	75.0	0.35

Diffusion driven by NaBr(3) concentration gradients

The D_{33} values plotted in Fig. 3 give the flux of NaBr produced by NaBr concentration gradients in DTAB + NaOct solutions without added NaBr. In the limit $f_1 = 0$, D_{33} is the tracer diffusion coefficient of Br$^-$ ions in 40 mmol dm^{-3} NaOct solution. In the other limiting case, $f_1 = 1.00$, D_{33} is the tracer diffusion coefficient of Na$^+$ ions 40 mmol dm^{-3} DTAB. Binding of Na$^+$ ions to cationic DTAB micelles is expected to be negligible. Indeed, the extrapolated $D_{33}(f_1 = 1.00)$ value, 1.35×10^{-5} cm^2 s^{-1}, is nearly identical to the diffusion coefficient of free Na$^+$ ions (1.33×10^{-5} cm^2 s^{-1}).[34]

Cross-coefficients D_{13} and D_{23} are small compared to the other cross-coefficients plotted in Fig. 3, which means that NaBr concentration gradients drive relatively weak coupled flows of DTAB and NaOct components. This result can be understood by noting that gradients in the concentration of NaBr have minor effects on the formation of micelles relative to effects caused by gradients in the DTAB and NaOct surfactants. Also, the difference in mobility between Na$^+$ and Br$^-$ ions is smaller than the difference in mobilities between micelles and counterions, so the electric field generated by NaBr concentration gradients are weaker.

The D_{ik} coefficients reported here were measured for aqueous DTAB(1) + NaOct(2) carrier solutions without added NaBr ($\bar{c}_3 = 0$). Nevertheless, it is still possible to have coupled flows of NaBr in these solutions, as indicated by the nonzero values of cross-coefficients D_{31} and D_{32}. In this case, the Na$^+$ and Br$^-$ ions for the coupled flows of NaBr are provided by the DTAB and NaOct components.

Nonlinear least-squares analysis

The precise evaluation of temporal moments becomes increasingly difficult for higher-order moments.[23] Small uncertainties in the baseline, for example, become magnified. Consequently, the relative precision of the X, Y, Z parameters derived from the second moments is poorer than that of the P, Q, S, E, F, G parameters evaluated from the peak heights and areas (see Table 3). Also, the precision of D_{ik} coefficients evaluated by moments analysis is generally poorer than that obtained by direct nonlinear least-squares analysis of dispersion profiles.

As mentioned in the Introduction, initial attempts to analyze the DTAB + NaOct profiles by nonlinear least-squares fitting failed to converge to the highly unusual peak shapes. Moments analysis, however, gives values for all nine quaternary D_{ik} coefficients for these solutions, from which the eigenvalues and eigenvectors of the $\boldsymbol{D}$ matrix can be evaluated together with the pre-exponential factors

$$w_i = \frac{\sum_{p=1}^{3}\sum_{q=1}^{3} R_p A_{pi} B_{iq} \Delta c_q}{\sum_{k=1}^{3}\sum_{p=1}^{3}\sum_{q=1}^{3} R_p A_{pk} B_{kq} \Delta c_q} \qquad (27)$$

This information provides very good initial estimates of the fitting parameters D_1, D_2, D_3, a, b, d, e, f, g required for nonlinear least-squares analysis of the profiles. For initial gradients only in $\bar{c}_1$ ($\Delta c_2 = \Delta c_3 = 0$), for example, the values of w_1, w_2, w_3 calculated from eqn. (27) are $a+b$, $e+f$,$1-a-b-e-f$, respectively. For initial gradients in $\bar{c}_2$ only ($\Delta c_1 = \Delta c_3 = 0$), the corresponding w_1, w_2, w_3 values are $a+d$, $e+g$, $1-a-d-e-g$, respectively. The expressions for these six w_i values are easily solved for a, b, d, e, f and g.

Using accurate initial parameter estimates provided by moments analysis, nonlinear least-squares fitting of the DTAB + NaOct dispersion profiles converged rapidly. The D_{ik} coefficients evaluated by nonlinear least-squares analysis are listed in Table 7. These D_{ik} values agree within experimental precision with the D_{ik} values from moments analysis (Table 5). As anticipated, the nonlinear least-squares D_{ik} values are more precise. However, both the moments analysis and the nonlinear least-squares fitting failed to converge to profiles measured for DTAB solute fractions near 0.25 owing to the near coincidence of eigenvalues D_2 and D_3.

Unusual shapes of DTAB + NaOct dispersion profiles

Finally, to explain the highly unusual shapes of the DTAB + NaOct profiles, Fig. 4 shows the concentration profiles for DTAB, NaOct, and NaBr produced by injecting excess NaOct into a 38.0 mmol dm^{-3} DTAB + 2.0 mmol dm^{-3} NaOct carrier solution. In this example, counter-current diffusion of DTAB driven by the NaOct gradient removes DTAB from the centre of the profile, producing a buildup of DTAB in the leading and trailing edges. Simultaneously, co-current coupled diffusion of NaBr driven by the NaOct gradient removes NaBr from the edges of the profile, leading to a buildup of NaBr at the center of the profile and a sharp central peak. The concentration profile of the injected NaOct superimposed on concentration profiles of DTAB and NaBr produced by coupled diffusion produces a refractive-index profile with three maxima and two minima (see Fig. 1).

Alternate descriptions of diffusion in aqueous DTAB + NaOct solutions

In this paper, diffusion in aqueous DTAB + NaOct solutions is described in terms of the fluxes of DTAB, NaOct and NaBr components. This is the logical choice of components for a discussion of the interactions between the fluxes of a cationic surfactant and an anionic surfactant. Also, NaBr is non-associating (which simplifies the discussion) and is readily available in pure form. It should be pointed out, however, that the description of diffusion in DTAB + NaOct solutions employed here is not unique. For this kind of mixed electrolyte (two univalent cations and two univalent anions), there are in fact four possible ways to choose the fluxes of three neutral electrolyte components (*i.e.*, fluxes of any three of the DTAB, NaOct, NaBr, and DTAOct components). For example, though less convenient, diffusion in DTAB + NaOct solutions could be described in terms of the fluxes of J_i' of DTAB($\bar{c}_1'$) + NaOct($\bar{c}_2'$) + DTAOct($\bar{c}_3'$) components. This alternate set of component fluxes is related to the fluxes J_i of the DTAB($\bar{c}_1$) + NaOct($\bar{c}_2$) + NaBr($\bar{c}_3$) components as follows: $J_1' = J_1 + J_3$, $J_2' = J_2 + J_3$, $J_3' = -J_3$. These relations can be used to transform the measured D_{ik} coefficients for the DTAB($\bar{c}_1$) + NaOct($\bar{c}_2$) + NaBr($\bar{c}_3$) components to the D_{ik} coefficients for the DTAB($\bar{c}_1'$) + NaOct($\bar{c}_2'$) + DTAOct($\bar{c}_3'$) components. Ref. 34 give details of the procedure for transforming D_{ik} coefficients from one set of components to another.

5. Conclusions

Quaternary mutual diffusion coefficients can be evaluated from the temporal moments of Taylor dispersion profiles. This method of analysis is recommended for dispersion profiles with complicated shapes produced by strongly coupled diffusion. These profiles are difficult to analyze by nonlinear least-squares procedures because accurate initial estimates of the fitting parameters are required for convergence. Moments analysis of dispersion profiles for aqueous DTAB + NaOct solutions provides detailed information about quaternary mutual diffusion in solutions of a cationic–anionic mixed surfactant. In these solutions the diffusion of each surfactant can produce a coupled flux of the other surfactant and a coupled flux of NaBr which exceeds its own flux.

Appendix

Moments analysis of Taylor dispersion data is based on the assumption of Gaussian profiles, which is not strictly correct. The following numerical procedure can be used to reduce errors from the Gaussian approximation to negligible levels and to simplify the evaluation of H', I_1', I_2'. The first step is to fit the accurate (non-Gaussian) dispersion equation

$$V(t) = B_0 + B_1 t + \sqrt{t_R/t}\sum_{i=1}^{N} V_i \exp[-a_i(t - t_R)^2 t_R/t] \quad \text{(A1)}$$

to the measured detector voltages, treating B_0, B_1 and V_1, V_2,... V_N as adjustable linear least-squares parameters. The values of a_i are calculated from a set of N "comb" diffusion coefficients $\mathcal{D}_i$ chosen to span the region from the smallest eigenvalue to the largest eigenvalue of the anticipated matrix of the D_{ik} coefficients: $a_i = 12\mathcal{D}_i/r^2 t_R$. For the DTAB + NaOct solutions, $\mathcal{D}_i/10^{-5}$ cm^2 s^{-1} values such as 0.06, 0.12,

Table 7 Quaternary mutual diffusion coefficients[a] for aqueous DTAB ($\bar{c}_1$) + NaOct($\bar{c}_2$) + NaBr($\bar{c}_3 = 0$) solutions at 25 °C from nonlinear least-squares analysis

$\bar{c}_1$/mmol dm^{-3}	2	20	30	38
$\bar{c}_2$/mmol dm^{-3}	38	20	10	2
$D_{11}/10^{-5}$ cm^2 s^{-1}	0.100 (0.006)	0.421 (0.011)	0.334 (0.020)	0.268 (0.002)
$D_{12}/10^{-5}$ cm^2 s^{-1}	−0.010 (0.004)	−0.100 (0.003)	−0.256 (0.002)	0.310(0.009)
$D_{13}/10^{-5}$ cm^2 s^{-1}	0.008 (0.002)	0.186 (0.004)	0.086 (0.002)	0.083 (0.002)
$D_{21}/10^{-5}$ cm^2 s^{-1}	−0.85 (0.03)	−0.320 (0.013)	0.018 (0.006)	0.0068(0.0005)
$D_{22}/10^{-5}$ cm^2 s^{-1}	0.85 (0.02)	0.248 (0.006)	0.206 (0.010)	0.164 (0.005)
$D_{23}/10^{-5}$ cm^2 s^{-1}	−0.129 (0.02)	−0.104 (0.005)	0.056 (0.005)	0.020 (0.002)
$D_{31}/10^{-5}$ cm^2 s^{-1}	1.57 (0.06)	0.531 (0.004)	0.077 (0.014)	0.007 (0.018)
$D_{32}/10^{-5}$ cm^2 s^{-1}	0.019 (0.016)	0.685 (0.007)	1.027 (0.021)	1.165 (0.012)
$D_{33}/10^{-5}$ cm^2 s^{-1}	1.777 (0.002)	1.380 (0.004)	1.341 (0.010)	1.334(0.003)

[a] Precision quoted as two standard deviations (in parentheses).

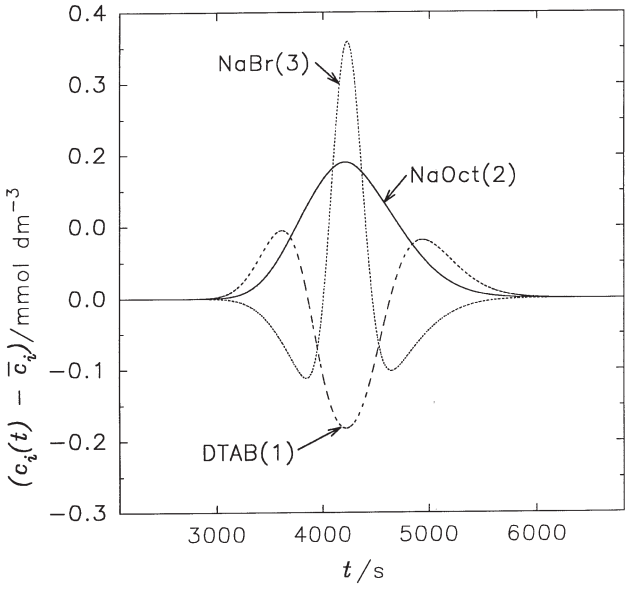

Fig. 4 Concentration profiles across a dispersion profile produced by injecting a solution sample containing a 20.0 mmol dm^{-3} excess of NaOct into a carrier stream containing 38.0 mmol dm^{-3} DTAB + 2.0 mmol dm^{-3} NaOct. The resulting refractive index profile has 3 maxima and two minima (curve c in Fig. 1).

0.24, 0.48, 0.96, 1.92 ($N = 6$) gave excellent initial fits. The retention time t_R was usually known to within ±30 s from the flow rate of the carrier solution and the internal volume of the dispersion tube. To evaluate accurate retention times, small adjustments to t_R were made for each profile to improve the fit of eqn. (A1) to the detector voltages. Subtracting the fitted baseline $B_0 + B_1 t$ gave the Gaussian profiles

$$^{E}V(t) = \sum_{i=1}^{N} V_i \exp[-a_i(t - t_R)^2]$$

and hence

$$H = \sum_{i=1}^{N} V_i$$

$$I_0 = \sqrt{\pi} \sum_{i=1}^{N} \frac{V_i}{\sqrt{a_i}}$$

$$I_1 = \sum_{i=1}^{N} \frac{V_i}{a_i}$$

$$I_2 = \sqrt{\frac{\pi}{2}} \sum_{i=1}^{N} \frac{V_i}{a_i \sqrt{a_i}}$$

The values of H, I_0, I_1 and I_2 calculated in this manner were used to evaluate a preliminary set of eigenvalues of the $\boldsymbol{D}$ matrix. The set of $Đ_i$ values was then refined to include these eigenvalues together with larger and smaller values of $Đ_i$ to serve as "guard" eigenvalues, and the calculation of H, I_0, I_1 and I_2 was repeated. Absolute values of the refractive-index increments R_i are not required for the moments analysis. Ignoring the detector sensitivity (a constant), accurate relative R_i values required for the evaluation α_1 and α_2 for each profile were obtained as linear least-squares parameters by fitting the equation $I_0 = R_1\Delta c_1 + R_2\Delta c_2 + R_3\Delta c_3$ to the peak areas.

To test the proposed moments analysis, simulated dispersion profiles were calculated using eqns. (4) and (5) for assumed sets of quaternary D_{ik} coefficients. The D_{ik} values recovered by moments analysis of the simulated profiles agreed with the correct D_{ik} values to within $\pm 0.001 \times 10^{-5}$ cm^2 s^{-1} or better.

Acknowledgements

Acknowledgment is made to the Natural Sciences and Engineering Research Council for the financial support of this research.

References

1 D. G. Leaist, *J. Colloid Interface Sci.*, 1986, **111**, 240.
2 D. G. Leaist and L. Hao, *J. Chem. Soc., Faraday Trans.*, 1995, **91**, 2837.
3 D. G. Leaist, *J. Solution Chem.*, 1991, **20**, 175.
4 D. G. Leaist, *Can. J. Chem.*, 1990, **68**, 33.
5 S. M. Abdu and D. G. Leaist, *J. Chem. Eng. Data*, 2001, **46**, 922.
6 K. MacEwan and D. G. Leaist, *J. Phys. Chem. B*, 2001, **105**, 690.
7 M. Castaldi, L. Constantino, O. Ortona, L. Paduano and V. Vitagliano, *Langmuir*, 1998, **14**, 5994.
8 K. MacEwan and D. G. Leaist, *J. Phys. Chem. B*, 2002, **106**, 10 296.
9 L. Constantino, C. D. Volpe, O. Ortona and V. Vitagliano, *J. Chem. Soc., Faraday Trans.*, 1992, **88**, 61.
10 D. G. Leaist and L. Hao, *J. Phys. Chem.*, 1995, **99**, 12 896.
11 D. G. Leaist, *Phys. Chem. Chem. Phys.*, 2002, **4**, 4732.
12 D. F. Evans and H. Wennerström, *The Colloidal Domain*, Wiley, New York, 2nd edn., 1999.
13 P. C. Hiemenz and R. Rajagopalan, *Principles of Colloid and Surface Chemistry*, Marcel Dekker, New York, 3rd edn. 1997.
14 E. Marques, A. Khan, M. da Graca Miguel and B. Lindman, *J. Phys. Chem.*, 1993, **97**, 4729.
15 M. Bergström, *Langmuir*, 2001, **17**, 993.
16 N. Filipovic-Vincekovic and D. Skrtic, *Colloid Polymer Sci.*, 1988, **266**, 954.
17 N. Kamenka, M. Chorro, Y. Talmon and R. Zana, *Colloids Surf.*, 1992, **67**, 213.
18 T. Kato, H. Takeuchi and T. Seimiya, *J. Phys. Chem.*, 1992, **96**, 6839.
19 L. Hao and D. G. Leaist, *J. Solution Chem.*, 1995, **24**, 523.
20 H. J. V. Tyrrell and K. R. Harris, *Diffusion in Liquids*, Butterworths, London, 1984.
21 D. G. Leaist, *Ber. Bunsenges. Phys. Chem.*, 1991, **95**, 117.
22 L. Hao and D. G. Leaist, *J. Solution Chem.*, 1993, **22**, 263.
23 L. Hao, D. G. Leaist and R. Ibrahimov, *J. Chem. Soc., Faraday Trans.*, 1993, **89**, 515.
24 Z. Deng and D. G. Leaist, *Can. J. Chem.*, 1991, **69**, 1548.
25 Z. Deng, H. Lü and D. G. Leaist, *J. Chem. Eng. Data*, 1996, **41**, 214.
26 R. H. Stokes, *J. Am. Chem. Soc.*, 1950, **72**, 2243.
27 D. G. Leaist, *J. Colloid Interface Sci.*, 1986, **111**, 230.
28 A. Siderius, S. Kolisnek Kehl and D. G. Leaist, *J. Solution Chem.*, 2002, **31**, 607.
29 P. J. Dunlop, *J. Phys. Chem.*, 1965, **69**, 4276.
30 H. D. Ellerton, G. Reinfelds, D. Mulcahy and P. J. Dunlop, *J. Phys. Chem.*, 1964, **68**, 403; D. G. Leaist, *J. Phys. Chem.*, 1990, **94**, 5180.
31 L. J. Gosting and D. F. Akeley, *J. Am. Chem. Soc.*, 1952, **74**, 2058.
32 P. Mukerjee and K. J. Mysels, *Critical Micelle Concentrations of Aqueous Surfactant Systems*, Natl. Stand. Ref. Data Series, Natl. Bur. Stand (U.S.), Washington, 1971.
33 R. A. Robinson and R. H. Stokes, *Electrolyte Solutions*, Butterworths, London, 2nd edn., 1959.
34 D. G. Leaist, *Ber. Bunsenges. Phys. Chem.*, 1985, **89**, 786.